

Coherent control of broadband isolated attosecond pulses in a chirped two-color laser field

Pu Zou, Zhinan Zeng, Yinghui Zheng, Yingying Lu, Peng Liu, Ruxin Li,* and Zhizhan Xu†

State Key Laboratory of High Field Laser Physics, Shanghai Institute of Optics and Fine Mechanics, Chinese Academy of Sciences, Shanghai 201800, People's Republic of China

(Received 2 January 2010; published 31 March 2010)

A theoretical investigation is presented that uses a strong two-color laser field composed of a linearly chirped fundamental (900 nm) and its subharmonic (1800-nm) laser pulses to control coherently the broadband isolated attosecond pulses in high-order harmonic generations. After the subharmonic field is added, the intrinsic chirp of harmonic emission can be reduced significantly, and consequently, the temporal synchronization of harmonic emission with different photon energies at the level of the single-atom response can be realized. In addition, the scheme is robust against the carrier envelope phase variation to produce a twin pulse of stable sub-100-as duration, and the relative intensity of the twin pulses can be changed just by adjusting the relative time delay of the two driving pulses, which is of benefit in general pump-probe experiments.

DOI: [10.1103/PhysRevA.81.033428](https://doi.org/10.1103/PhysRevA.81.033428)

PACS number(s): 32.80.Qk, 42.65.Re, 33.20.Xx

I. INTRODUCTION

Isolated attosecond pulses (IAPs) are powerful tools for studying electron dynamics with unprecedented time scales in atoms. Until now, high-order harmonic generation (HHG) has been the only method that has produced IAPs [1–4] experimentally. Recently, isolated 80-as pulses were obtained by selecting cutoff harmonics generated by a 3.3-fs linearly polarized fundamental pulse with a stabilized carrier envelope phase (CEP) [1]. With this technique, the pulse duration achievable is limited by the bandwidth of the continuum, which is less than 20 eV [2]. Needless to say, the generation of near-one-optical-cycle pulses that contain enough energy to excite HHG is an extremely difficult task. An alternative approach to the generation of IAP involves the polarization gating (PG) technique [5]. Experimentally, PG pulses have been generated by combining two counter-rotating circularly polarized laser pulses with a proper delay [6–9]. However, because of the depletion of the ground-state population of the atom by the leading edge of the laser pulse, the PG duration is limited to about a fifth of the duration of the excitation pulse [9]. Recently, the double optical gating technique for generating IAPs with multicycle lasers has been demonstrated, combining PG and two-color gating [10–12]. Although a nearly 170-eV-wide extreme ultraviolet (XUV) supercontinuum spectrum corresponds to IAPs, owing to the limitation to the bandwidth of the Mo/Si mirror and residual pulse dispersion, only a portion of the spectrum was used to generate isolated 107-as XUV pulses [12].

In addition, a two-color scheme using the fundamental and its second harmonic controlling pulses has been theoretically proposed as an efficient method to generate IAP [13–15], which also has been experimentally demonstrated recently [16,20]. In fact, there are more advantages in using a subharmonic than a second harmonic as controlling field [17,18]. First, a more broadband supercontinuum can be generated by adding a subharmonic controlling field than a second harmonic controlling field. Since according to the three-step

model [19], the ponderomotive energy and the spectral cutoff are proportional to the wavelength squared, the longer driving wavelengths will generate higher-order harmonics. In addition, by adding a subharmonic controlling field, the duration of the driving pulse can even be doubled, which enables the generation of a broadband supercontinuum in the multicycle regime [17]. Experimentally, these features have been proved by Vozzi *et al.* [20]. In their experiment, a broader XUV continuum, extending beyond 100 eV, was observed in argon, and a continuous XUV spectrum extending from 36 to 70 eV was generated in krypton.

However, the shortest IAP duration attainable is further limited by the intrinsic chirp of the harmonic emission, which is originated from the laser-intensity-dependent atomic dipole phase [21,22]. Consequently, the phase control and chirp compensation of attosecond harmonic pulses are of vital importance for producing Fourier-limited (FL) attosecond pulses. Continuing efforts in phase control and chirp compensation of attosecond harmonic pulses have recently led to the breakthroughs of producing nearly FL attosecond pulse trains [23–26]. Zheng *et al.* [26] proposed a scheme to compensate dynamically for the intrinsic chirp of attosecond harmonic pulses. In their experiment, by adding a weak second harmonic laser field to the driving laser field, the chirp compensation can be varied from the negative to the positive continuously by simply scanning the relative time delay between the two-color pulses. As a result, a nearly FL attosecond pulse train was produced in the XUV region.

In this work, we propose a different method for compensation of the negative chirp of IAPs in the water window spectral region (281–539 eV) using a chirped two-color field. To compensate for the intrinsic negative chirp of the harmonic in the supercontinuum region of 304–373 eV, the fundamental driving pulse has a proper positive linear chirp, and for controlling the electronic dynamics in HHG, a subharmonic in a multicycle regime is synthesized with the fundamental field. Consequently, by simply adjusting the relative time delay between the two-color pulses, an IAP with a duration of 69 as, which is close to the FL value of 53 as, was generated. In addition, the cutoff energy of the harmonic could be extended to 386 eV and a broadband supercontinuum spectrum with a bandwidth of 97 eV in the water window region can be

*ruxinli@mail.shnc.ac.cn

†zzxu@mail.shnc.ac.cn

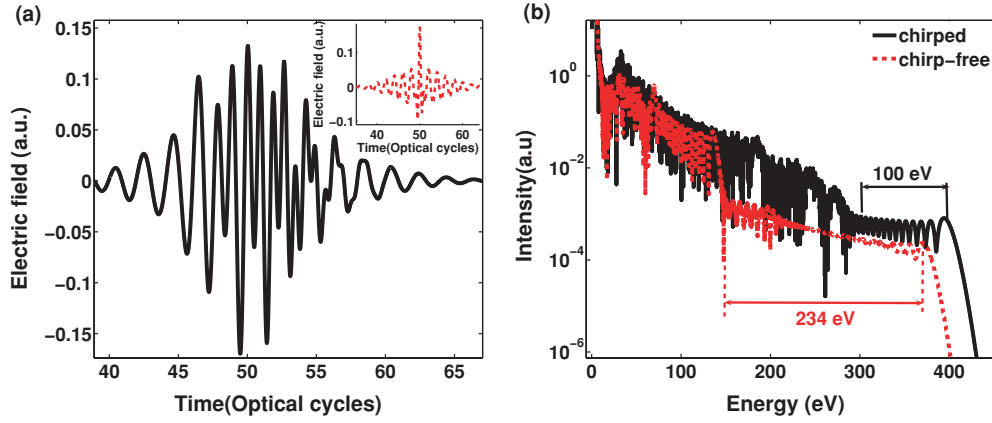


FIG. 1. (Color online) (a) Electric field of the chirped two-color field (solid curve) with time delay $t_0 = -1312.5$ as. Inset: electric field of the two-color field without chirp (dashed curve). (b) Harmonic spectrum corresponding to the chirped two-color field (solid curve) shown in (a), and harmonic spectrum (dashed curve) generated by the chirp-free two-color field shown in inset to (a).

generated. Surprisingly, if the intensity of the subharmonic field is increased, an IAP with a duration of 57 as can be obtained directly, which is much closer to the FL value. Furthermore, the scheme is robust against the CEP variation to produce a twin pulse with a stable sub-100-as duration, which can be efficiently applied to control HHG in the time domain.

II. MODEL AND NUMERICAL METHOD

To demonstrate our method theoretically, the single-atom response was calculated with the nonadiabatic Lewenstein model [27], which is based on a single-active-electron model and has been widely used. The model atom in the calculations is helium (He). The atomic dipole moment is calculated using Eq. (1) in Ref. [28] and the harmonic spectrum is obtained by Fourier transforming the time-dependent dipole moment. The expression for the two-color field is

$$E_s = E_1 \exp[-2 \ln(2)t^2 / N^2 \tau_1^2] \cos[\omega t + \phi(t) + \delta_{\text{CEP}}] \\ + E_2 \exp[-2 \ln(2)(t + t_0)^2 / \tau_2^2] \\ \times \cos[0.5\omega(t + t_0) + 0.5\delta_{\text{CEP}}]. \quad (1)$$

In Eq. (1), $\phi(t)$ is the phase induced by the linear chirp, which can be written as

$$\phi(t) = \pm 2 \ln(2) \sqrt{N^2 - 1} t^2 / (N^2 \tau_1^2) \quad (2)$$

Here E_i and τ_i ($i = 1, 2$) are the amplitude and duration for the fundamental and subharmonic pulses, respectively. The t_0 in Eq. (1) denotes the relative time delay between the two pulses. ω and δ_{CEP} are the angular frequency and the CEP of the fundamental pulses, respectively. N is a parameter for controlling the linear chirp of the fundamental pulse. The peak intensity, full-width half-maximum (FWHM) duration, and central wavelength of the laser pulses are 5.0×10^{14} W/cm², 3 fs, and 900 nm for the fundamental pulses, which so far are difficult to obtain. However, when a proper positive chirp is added, that is, $N = 5$, the pulse duration is expanded to 15 fs. It is lucky that spectra broad enough to support pulses < 5 fs can be easily obtained by the hollow-fiber or filament technique [29], and thus a 15-fs pulse with a proper positive chirp is achievable using state-of-the-art pulse compression

technology. The peak intensity, FWHM duration, and central wavelength of the subharmonic pulses are 1.0×10^{14} W/cm², 30 fs, and 1800 nm, respectively.

III. RESULTS AND DISCUSSIONS

The typical electric fields of the chirped and chirp-free two-color pulses are shown in Fig. 1(a). It shows that the difference between the highest and the second-highest half-cycle cutoff photon energies in the chirp-free field (dashed curve in inset to Fig. 1) is much larger than that in the chirped two-color field (solid curve); consequently, from the semiclassical three-step model point, a broadband XUV supercontinuum with a bandwidth of nearly 234 eV (152–386 eV), shown in Fig. 1(b) (dashed curve), is generated when the time delay $t_0 = -187.5$ as in the chirp-free case, while a supercontinuum with a bandwidth of only 100 eV (solid curve) can be obtained in the chirped two-color case when the time delay $t_0 = -1312.5$ as. In addition, also shown in Fig. 1(b), the intensity of the supercontinuum spectrum is increased by nearly 1 order of magnitude when the fundamental pulse is chirped. However, the entire supercontinuum with a bandwidth of 234 eV cannot support a sub-100-as IAP directly because of its intrinsic chirp, as harmonics with different energies have different emission times in the three-step model; that is, high harmonics are not synchronized on an attosecond time scale, thus setting a lower limit to the achievable duration. Then by simply making an inverse Fourier transformation of the XUV supercontinuum in the 69-eV spectral width (selected with a numerical spectral filter ranging from 304 to 373 eV) shown in the top plot in Fig. 2(a), without employing phase compensation, an isolated 111-as pulse can be obtained, as shown in the bottom plot in Fig. 2(a) (solid curve). If the intrinsic chirp is well compensated for, a single FL 53-as pulse with a clean time profile can be obtained [dashed curve in Fig. 2(a)].

To obtain an IAP with a much shorter duration, the fundamental driving pulse is properly positively linearly chirped in two-color pulses, shown by the solid curve in Fig. 1(a). The optimal value of the linear chirp induced onto the fundamental laser pulse appears at $N = 5$; that is, the

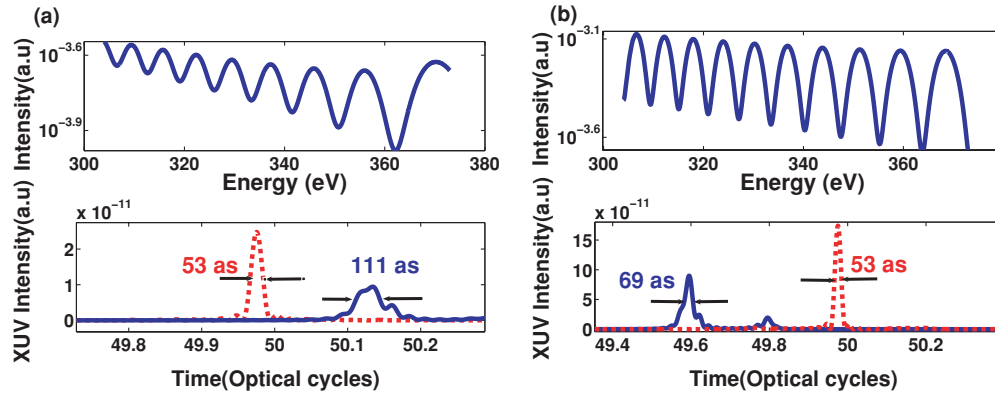


FIG. 2. (Color online) (a) Top: supercontinuum with a bandwidth of 69 eV generated by the two-color field with a relative time delay $t_0 = -187.5$ as without chirp [$N = 1$ in Eq. (2)]. Bottom: temporal characteristics of the spectrum shown in the top curve. IAPs are obtained with [dashed (red) curve] and without [solid (blue) curve] phase compensation assumed in the simulation. (b) Top: supercontinuum with a bandwidth of 69 eV generated by the two-color field of relative time delay $t_0 = -1312.5$ as with chirp [$N = 5$ in Eq. (1)]. Bottom: temporal characteristics of the spectrum shown in the top curve. IAPs are obtained with [dashed (red) curve] and without [solid (blue) curve] phase compensation assumed in the simulation.

FWHM duration is expanded to 15 fs, while the peak intensity is unchanged. As a result, obviously, as shown in Fig. 1(b), not only is the cutoff energy of the supercontinuum spectrum (solid curve) extended compared to that (dashed curve) in the chirp-free case, but also the duration of the IAP is significantly reduced, as shown in Fig. 2(b) (solid curve), compared to that in Fig. 2(a) (solid curve). In addition, we noticed that the modulation depth of the harmonic spectrum in Fig. 2(b) is larger than that in Fig. 2(a), which due to the interferences of the two contributing quantum paths, are different in these two cases. Moreover, it is clear that a satellite pulse appears at $t = 49.8T_0$ (T_0 is the optical cycle of the fundamental pulse) shown in Fig. 2(b), corresponding to the long quantum path, which can easily be eliminated through phase matching in experiments. In our simulation, we found that the optimal time delay for pulse compression is about $t_0 = -1.3125$ fs, which makes the two-color scheme with an 1800-nm controlling pulse an attractive candidate for generation of sub-100-as IAPs.

Figure 3 shows the harmonics emission times, that is, $t_e + NT(\omega_q)$, for the supercontinua generated in HHG, in which $T(\omega_q)$ is the intrinsic time period at harmonic frequency ω_q and N is an integer. The spectral phase $\varphi(\omega_q)$, which is sampled only at harmonic frequencies ω_q , reflects their synchronization during the emission process. As we know that a linear relationship $\varphi(\omega_q) = q\omega_0 t_e$, with t_e independent of q , results in so-called FL pulses of a duration that is the shortest allowed by the bandwidth. In that case, all harmonics are emitted at the same time, $t_e = \Delta\varphi/(2\omega_0)$ [21]. Because of the uncertainty principle, one cannot define an instant associated with a single energy: the emission time of harmonic q applies to a group of harmonics centered on ω_q , which is the group delay dispersion. In Fig. 3, $\Delta\varphi$ is a relative value, thus the effective part for characterizing the intrinsic harmonic chirp is the slope of the spectral phase difference, the so-called the second-order spectral phase. So by adding 2π multiplied by the appropriate integers N , the phases corresponding to the sampled harmonic order (220th–270th in this case) can

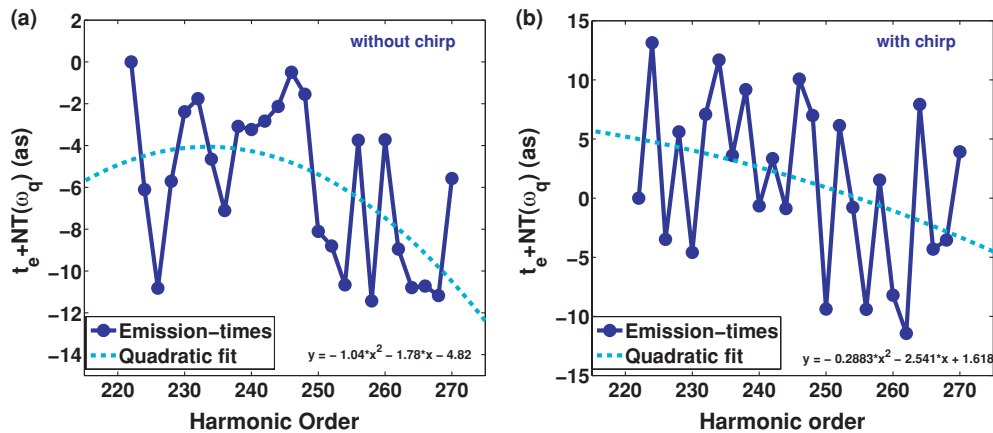


FIG. 3. (Color online) Harmonics emission times for the supercontinuum generated by (a) chirp-free two-color pulses and (b) chirped two-color pulses. Filled circles, spread and chirp for emission times $t_e + NT(\omega_q)$; dashed lines, quadratic fit. Quadratic fitting equations are shown. Parameters are the same as in Fig. 2.

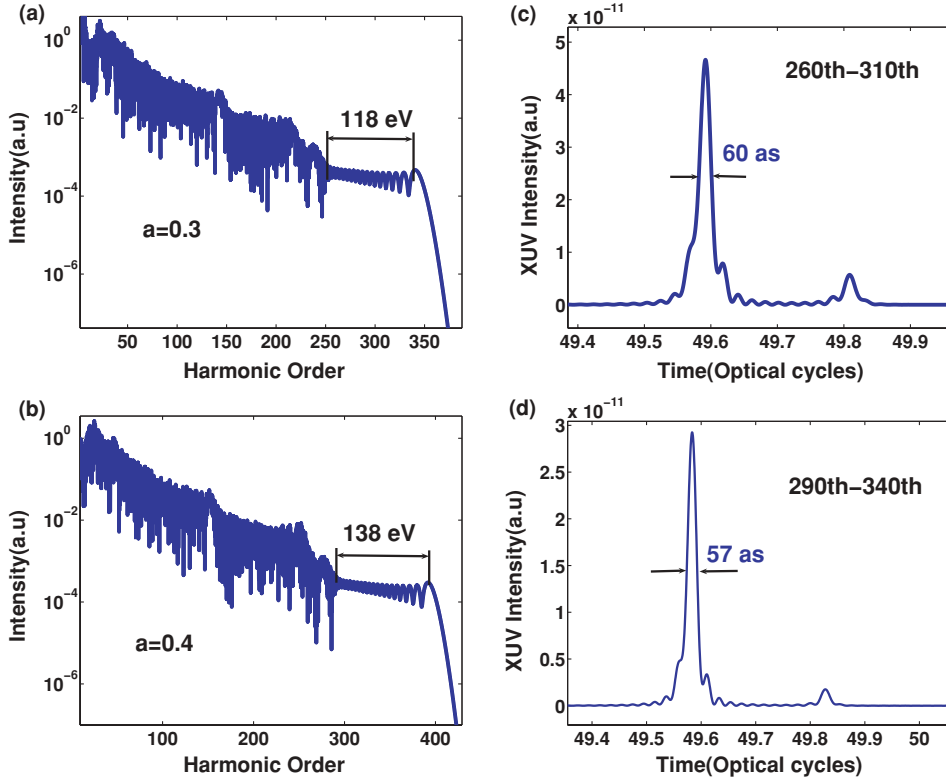


FIG. 4. (Color online) Harmonic spectra of helium atoms driven by chirped two-color fields with different relative intensities when (a) $a = 0.3$ and (b) $a = 0.4$. (b, c) Corresponding IAPs. The peak intensity of the chirped fundamental field is $5.0 \times 10^{14} \text{ W/cm}^2$. CEPs of the subharmonic and the fundamental fields are 0.

be brought to more or less follow a straight line. Then by subtracting the time delay of the attosecond pulses, the spread and chirp of the emission times $t_e + NT(\omega_q)$ can be obtained directly as shown in Fig. 3 (filled circles). In Fig. 3(a) the negative slope of the fitting curve indicates that the harmonic pulses are negative chirp in the chirp-free two-color field. In this case, the second-order spectral phase, calculated by the slope of the quadratic fit from the 220th (304-eV) to the 270th (373-eV) order is $-3.4 \times 10^{-3} \text{ fs}^2$ at a delay of -187.5 as , and the single-atom predicts of the chirp rate, that is, $C = \Delta t_e / \Delta E$, where E , the energy of the harmonics, is -5.113 as/eV [30]. For comparison, after the fundamental pulse is chirped, the calculated second-order spectral phase in the same energy region is $-1.7 \times 10^{-3} \text{ fs}^2$ and the corresponding chirp rate is -2.613 as/eV . It is obvious that not only is the absolute value of the chirp rate distinctly reduced, but also the dashed curve representing the harmonics emission time in Fig. 3(b) is nearly linear, which indicates that all harmonics in the spectral region of 304–373 eV are emitted at almost the same time. This available much shorter duration of an IAP, as shown in the bottom plot in Fig. 2(b) (solid curve), demands that this linearity be held for a much wider spectral range. The time delay between the chirped fundamental and the subharmonic field in our scheme is a vital parameter to compensate for the intrinsic chirp of the supercontinuum. As the intensity of the chirped two-color field is lower than the saturation intensity for a helium atom, the harmonic efficiency is mainly administered by the ionization rate according to the three-step model. Through a great deal of calculation, we found that the impact of the relative time delay between the two-color pulses is crucial to the ionization rate of ionized electrons, which results in two different harmonic spectral structures for

two time delays. Furthermore, our calculations show that an IAP with a duration of $<100 \text{ as}$ can hold when a time delay from $-0.5T_0$ (-1500 as) to $-0.3125T_0$ (-937.5 as) is chosen, which ensures that the scheme can be implemented much more easily in experiments.

The harmonic spectra as well as the corresponding attosecond pulses from a chirped two-color field of different relative intensities were also investigated (Fig. 4). The peak intensity of the chirped fundamental field remains $I_1 = 5.0 \times 10^{14} \text{ W/cm}^2$. The CEPs of both the fundamental and the subharmonic fields are 0. The relative time delay between two-color pulses remains $t_0 = -1312.5 \text{ as}$. As the relative intensity ratio $a = I_2/I_1$ increases from 0.3 to 0.4, the entire bandwidth of the supercontinuum increases from 118 to 138 eV, as shown in Figs. 4(a) and 4(b). By selecting harmonics from the 260th to the 310th (359–428 eV) and from the 290th to the 340th (400–469 eV), respectively, the corresponding obtainable durations of IAPs changed little, from 60 to 57 as, as shown in Figs. 4(c) and 4(d), respectively. Therefore, variation of the intensity of the subharmonic field does not change the generation of broadband supercontinua, which is good for experiments. Figure 5 shows the temporal profiles of the attosecond pulses generated by the harmonics with different central frequencies. It is shown in Fig. 5 that with an increase in the harmonic order, the interval between the emission times of the two pulses become smaller, which indicates that harmonics above the 200th are synchronized. This is another proof of the chirp compensation in our scheme. Although there are twin pulses between $49.5T_0$ and $49.9T_0$, the intensities of pulses emitted later are much weaker than those of the earlier pulses, thus the earlier ones can be ignored. This finding enables generation of sub-100-as close-to-FL IAPs

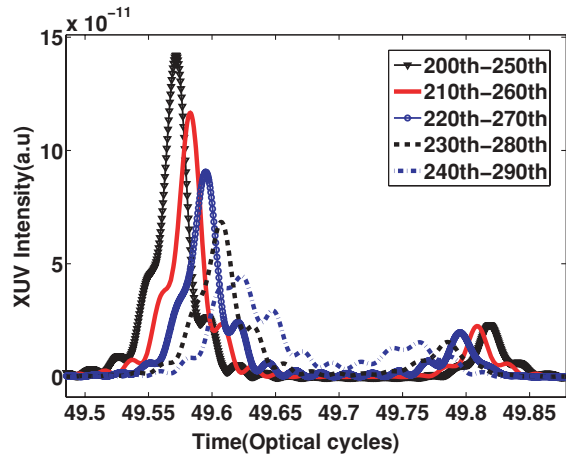


FIG. 5. (Color online) Temporal profiles of attosecond pulses generated by the harmonics with different central frequencies in the chirped two-color field. Parameters are the same as in Fig. 2(b).

with extremely short and tunable central wavelengths, which may play a vital role in controlling and investigating core-level dynamics inside atoms.

To explore the effects of the CEP on the formation of attosecond pulses in our scheme, we investigated the time profiles of harmonics in the fixed spectral region (230th–270th) near the cutoff obtained by inversely Fourier transforming the corresponding spectra. Figure 6 shows the temporal profiles of the harmonics spectra under the different CEPs of the chirped few-cycle fundamental driving laser pulses. Note that in the few-cycle regime, the CEP plays a crucial role in controlling the electron dynamics. Variation of the CEP for the chirped fundamental few-cycle driving field will not change the two-color pulse profiles dramatically. The curves shown in Fig. 6 indicate that the twin pulses, the duration of which is retained at 70 as for the higher-intensity one, and at 79 as for the other, can be generated without the effects of the CEP. The twin pulses with a fixed time interval (600 as)

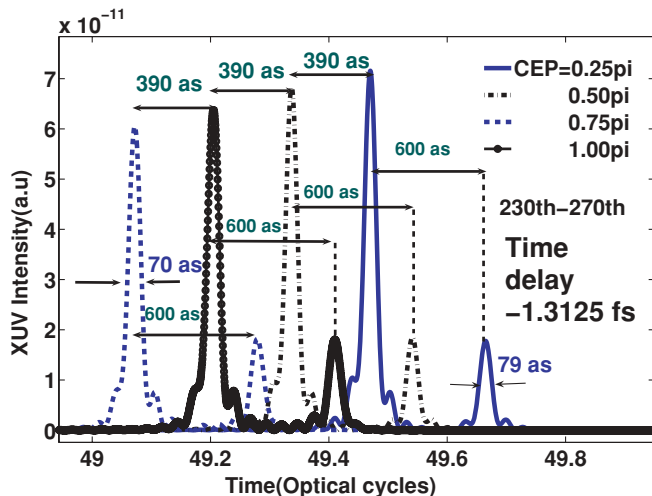


FIG. 6. (Color online) Temporal profiles of the supercontinua from 317 to 373 eV when the CEP of the chirped fundamental pulse is varied from 0.25π to π in the two-color field. The relative time delay in these cases was fixed at $t_0 = -1312.5$ as.

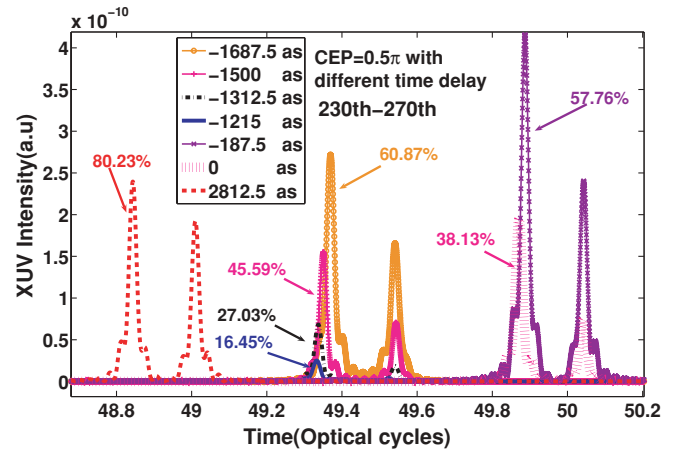


FIG. 7. (Color online) Temporal profiles of the supercontinua from 230th to 270th (317 to 373 eV) when the time delay of the two driving pulses was adjusted from -1687.5 to 2812.5 as. CEPs in these cases were kept at $\delta_{\text{CEP}} = 0.5\pi$. The percentage denotes the ratio of intensity of the second highest peak to the highest peak in a twin pulse.

and changeable relative intensity ratios can be employed as an efficient and simple tool in a pump-probe experiment. For example, we also did some calculations with changes in the relative intensity of the twin pulses by simply adjusting the relative time delay of the two driving pulses while keeping the CEP constant at 0.5π . The results are shown in Fig. 7. The percentage in Fig. 7 denotes the ratio of the intensity of the second-highest peak to that of the highest peak in the twin pulses for a certain time delay. Note that the relative intensity of the twin pulses can be adjusted from 16.45% [solid (blue) curve] to 80.23% [dashed (red) curve], which is obviously beneficial in general pump-probe experiments. Therefore, our two-color scheme, robust to CEP variation, can be efficiently applied to control HHG in the time domain. Furthermore, we can easily eliminate pulses of a lower intensity originated from the long quantum path, through phase matching by putting the gas cell at a proper distance after the laser focusing position, and consequently obtain the IAP efficiently.

The fundamental pulse with a duration of 3 fs is critical in our scheme. Recently, such a sub-1.5-cycle near-infrared light has been utilized for generation of robust, energetic, isolated sub-100-as pulses of XUV radiation [1]. However, at millijoule pulse energies, broadened spectra supporting pulses with a chirp of 15 fs can be generated by utilizing hybrid chirped mirror/prism compressor [29]. So we consider that it will not be difficult to generate a chirped few-cycle near-infrared pulse at 900 nm with a moderate intensity in the laboratory in the near future. An 1800-nm midinfrared pulse can be produced experimentally via an optical parametric amplifier.

IV. CONCLUSION

We have shown that the phase compensation of an IAP in the water window region can be achieved in a two-color laser field, from which we have demonstrated not only that an intense 69-as XUV IAP (with a bandwidth of 69 eV at a central wavelength of 3.67 nm) can be obtained directly in helium gas

by superimposing a subharmonic pulse on a positively chirped few-cycle fundamental pulse, but also that the absolute value of the chirp rate of the harmonic emission can be reduced from 5.113 to 2.613 as/eV in the water window spectral region of 304–373 eV. In addition, sub-100-as twin pulses with a fixed time interval and nearly constant intensity ratio can be obtained when the CEP of the few-cycle fundamental pulses is changed in our two-color scheme, which is an attractive candidate for pump-probe experiments. Furthermore, by increasing the intensity of the subharmonic field properly, an isolated 57-as pulse with the same bandwidth of 69 eV at a shorter central wavelength (2.85 nm) can be obtained, which is much closer to the FL value of 53 as. In addition, from the application point of view, the scheme using the subharmonic pulse rather than the second harmonic pulse relaxes the crucial requirements such as the precision of the time delay between the two pulses

and the robustness against CEP variation for the generation of stable twin attosecond pulses, which will greatly simplify the experimental arrangement. In addition, we found, through some calculations, that by changing the relative time delay in the chirped two-color pulses, the relative intensity of twin-pulses can also be varied over a large range, which is beneficial in general pump-probe experiments.

ACKNOWLEDGMENTS

This work was supported by the Chinese Academy of Science, National Natural Science Foundation (Grant Nos. 10734080, 10523003, 60921004, 10904157, and 60978012), the 973 Project (Grant No. 2006CB806000), and the Shanghai Commission of Science and Technology (Grant Nos. 06DZ22015 and 07PJ14091).

-
- [1] E. Goulielmakis, M. Schultze, M. Hofstetter, V. S. Yakovlev, J. Gagnon, M. Uiberacker, A. L. Aquila, E. M. Gullikson, D. T. Attwood, R. Kienberger, F. Krausz, and U. Kleineberg, *Science* **320**, 1614 (2008).
 - [2] A. Baltuska, Th. Udem, M. Uiberacker, M. Hentschel, E. Goulielmakis, Ch. Gohle, T. Holzwarth, V. S. Yakovlev, A. Scrinzi, T. W. Hansch, and F. Krausz, *Nature (London)* **421**, 611 (2003).
 - [3] M. Hentschel, R. Kienberger, Ch. Spielmann, G. A. Reider, N. Milosevic, T. Brabec, P. Corkum, U. Heinzmann, M. Drescher, and F. Krausz, *Nature (London)* **414**, 509 (2001).
 - [4] R. Kienberger, M. Hentschel, M. Uiberacker, Ch. Spielmann, M. Kitzler, A. Scrinzi, M. Weiland, Th. Westerwalbesloh, U. Kleineberg, U. Heinzmann, M. Drescher, and F. Krausz, *Science* **297**, 1144 (2002).
 - [5] P. B. Corkum, N. H. Burnett, and M. Y. Ivanov, *Opt. Lett.* **19**, 1870 (1994).
 - [6] V. Platonenko and V. Strelkov, *J. Opt. Soc. Am. B* **16**, 435 (1999).
 - [7] O. Tcherbakoff, E. Mevel, D. Descamps, J. Plumridge, and E. Constant, *Phys. Rev. A* **68**, 043804 (2003).
 - [8] B. Shan, S. Ghimire, and Z. Chang, *J. Mod. Opt.* **52**, 277 (2005).
 - [9] Z. Chang, *Phys. Rev. A* **70**, 043802 (2004).
 - [10] H. Mashiko, S. Gilbertson, C. Li, S. D. Khan, M. M. Shakya, E. Moon, and Z. Chang, *Phys. Rev. Lett.* **100**, 103906 (2008).
 - [11] H. Wang, M. Chini, S. D. Khan, S. Chen, S. Gilbertson, X. Feng, H. Mashiko, and Z. Chang, *J. Phys. B* **42**, 134007 (2009).
 - [12] H. Mashiko, S. Gilbertson, M. Chini, X. Feng, C. Yun, H. Wang, S. D. Khan, S. Chen, and Z. Chang, *Opt. Lett.* **34**, 3337 (2009).
 - [13] T. Pfeifer, L. Gallmann, M. J. Abel, D. M. Neumark, and S. R. Leone, *Opt. Lett.* **31**, 975 (2006).
 - [14] Z. Zeng, Y. Cheng, X. Song, R. Li, and Z. Xu, *Phys. Rev. Lett.* **98**, 203901 (2007).
 - [15] H. Merdji, T. Auguste, W. Boutu, J.-P. Caumes, B. Carre, T. Pfeifer, A. Jullien, D. Neumark, and S. Leone, *Opt. Lett.* **32**, 3134 (2007).
 - [16] Y. Zheng, Z. Zeng, X. Li, X. Chen, P. Liu, H. Xiong, H. Lu, S. Zhao, P. Wei, L. Zhang, X. Wang, J. Liu, Y. Cheng, R. Li, and Z. Xu, *Opt. Lett.* **33**, 234 (2008).
 - [17] P. Lan, P. Lu, W. Cao, Y. Li, and X. Wang, *Phys. Rev. A* **76**, 011402 (2007).
 - [18] W. Hong, Y. Li, P. Lu, P. Lan, Q. Zhang, and X. Wang, *J. Opt. Soc. Am. B* **25**, 1684 (2008).
 - [19] P. B. Corkum, *Phys. Rev. Lett.* **71**, 1994 (1993).
 - [20] C. Vozzi, F. Calegari, F. Frassetto, L. Poletto, G. Sansone, P. Villoresi, M. Nisoli, S. De. Silvestri, and S. Stagira, *Phys. Rev. A* **79**, 033842 (2009).
 - [21] Y. Mairesse, A. de Bohan, L. J. Frasinski, H. Merdji, L. C. Dinu, P. Monchicourt, P. Breger, M. Kovacev, R. Taïeb, B. Carré, H. G. Muller, P. Agostini, and P. Salières, *Science* **302**, 1540 (2003).
 - [22] T. Sekikawa, T. Ohno, T. Yamazaki, Y. Nabekawa, and S. Watanabe, *Phys. Rev. Lett.* **83**, 2564 (1999).
 - [23] A. Morlens, P. Balcou, P. Zeitoun, C. Valentin, V. Laude, and S. Kazamias, *Opt. Lett.* **30**, 1554 (2005).
 - [24] R. López-Martens, K. Varju, P. Johnsson, J. Mauritsson, Y. Mairesse, P. Salieres, M. B. Gaarde, K. Schafer, A. Persson, S. Svanberg, C. G. Wahlstrom, and A. L'Huillier, *Phys. Rev. Lett.* **94**, 033001 (2005).
 - [25] K. T. Kim, K. S. Kang, M. N. Park, T. Imran, G. Umesh, and C. H. Nam, *Phys. Rev. Lett.* **99**, 223904 (2007).
 - [26] Y. Zheng, Z. Zeng, P. Zou, Li Zhang, X. Li, P. Liu, R. Li, and Z. Xu, *Phys. Rev. Lett.* **103**, 043904 (2009).
 - [27] M. Lewenstein, P. Balcou, M. Y. Ivanov, A. L'Huillier, and P. B. Corkum, *Phys. Rev. A* **49**, 2117 (1994).
 - [28] T. Brabec and F. Krausz, *Rev. Mod. Phys.* **72**, 545 (2000).
 - [29] A. L. Cavalieri, E. Goulielmakis, B. Horvath, W. Helm11, M. Schultze, M. Fieß, V. Pervak, L. Veisz, V. S. Yakovlev, M. Uiberacker, A. Apolonski, F. Krausz, and R. Kienberger, *New J. Phys.* **9**, 242 (2007).
 - [30] S. Kazamias and Ph. Balcou, *Phys. Rev. A* **69**, 063416 (2004).